

# International Conference on Space Optics—ICSO 2010

Rhodes Island, Greece

4–8 October 2010

*Edited by Errico Armandillo, Bruno Cugny,  
and Nikos Karafolas*



## *Space evaluation of a MOEMs device for space instrumentation*

*Frederic Zamkotsian, Kyrre Tangen, Patrick Lanzoni,  
Emmanuel Grassi, et al.*



International Conference on Space Optics — ICSO 2010, edited by Errico Armandillo, Bruno Cugny,  
Nikos Karafolas, Proc. of SPIE Vol. 10565, 1056521 · © 2010 ESA and CNES  
CCC code: 0277-786X/17/\$18 · doi: 10.1117/12.2309205

## SPACE EVALUATION OF A MOEMS DEVICE FOR SPACE INSTRUMENTATION

Frederic Zamkotsian<sup>1</sup>, Kyrre Tangen<sup>2</sup>, Patrick Lanzoni<sup>1</sup>, Emmanuel Grassi<sup>1</sup>, Rudy Barette<sup>1</sup>, Christophe Fabron<sup>1</sup>, Luca Valenziano<sup>3</sup>, Laurent Marchand<sup>4</sup>, Ludovic Duvet<sup>4</sup>

<sup>1</sup> *Laboratoire d'Astrophysique de Marseille, CNRS, 38 rue Frederic Joliot Curie, 13388 Marseille Cedex 13, France*

<sup>2</sup> *Visitech, Kjellstadveien 5, Lier, P.O.Box 616, N-3003 Drammen, Norway*

<sup>3</sup> *INAF/IASF Bologna, via P. Gobetti 101, I-40129 Bologna, Italy*

<sup>4</sup> *European Space Agency, Keplerlaan 1, 2200 AG, Noordwijk, The Netherlands*

*E-mail address: frederic.zamkotsian@oamp.fr*

### I. INTRODUCTION

Large field of view surveys with a high density of objects such as high-z galaxies or stars benefit of multi-object spectroscopy (MOS) technique. This technique is the best approach to eliminate the problem of spectral confusion, to optimize the quality and the SNR of the spectra, to reach fainter limiting fluxes and to maximize the scientific return. Next generation MOS for space like the Near Infrared Multi-Object Spectrograph (NIRSpec) for the James Webb Space Telescope (JWST) require a programmable multi-slit mask. The European EUCLID mission has also considered a MOS instrument in its early study phase. Conventional masks or complex fiber-optics-based mechanisms are not attractive for space. The programmable multi-slit mask requires remote control of the multi-slit configuration in real time. A promising possible solution is the use of MOEMS devices such as micromirror arrays (MMA) [1,2,3] or micro-shutter arrays (MSA) [4]. MMAs are designed for generating reflecting slits, while MSAs generate transmissive slits. MSA has been selected to be the multi-slit device for NIRSpec and is under development at NASA's Goddard Space Flight Center. In Europe, an effort is currently under way to develop single-crystalline silicon micromirror arrays for future generation infrared multi-object spectroscopy [5]. By placing the programmable slit mask in the focal plane of the telescope, the light from selected objects is directed toward the spectrograph, while the light from other objects and from the sky background is blocked.

Visitech is an engineering company experienced in developing DMD solution for industrial customers. The Laboratoire d'Astrophysique de Marseille (LAM) has, over several years, developed different tools for modeling and characterization of MOEMS-based slit masks, especially during the design studies on JWST-NIRSpec [6,7]. ESA has engaged with Visitech and LAM in a technical assessment of using a Digital Micromirror Devices (DMD) from Texas Instruments for space applications (for example in ESA EUCLID mission). The DMD features 2048 x 1080 mirrors on a 13.68 $\mu$ m mirror pitch (left-hand side of Fig. 1). Typical operational parameters of this device are room temperature, atmospheric pressure and mirrors switching thousands of times in a second, while for MOS applications in space, the device should work in vacuum, at low temperature, and each MOS exposure would last for typically 1500s with micromirrors held in a static state (either ON or OFF) during that duration. A specific thermal / vacuum test chamber has been developed for test conditions down to -40°C at 10<sup>-5</sup> mbar vacuum. Imaging capability for resolving each micro-mirror has also been developed for determining any single mirror failure. Dedicated electronics and software allows us to hold any pattern on the DMD for duration of up to 1500s.

We present the summary of this ESA study, the electronic test vehicle as well as the cold temperature test set-up we have developed. Then, results of tests in vacuum at low temperature, including low temperature stress test, low temperature nominal test, thermal cycling, and life test are presented. Results after radiation (TID and proton), and vibration and shock are also shown.

### II. THE ELECTRONIC TEST VEHICLE

The DMD driver electronics consists of a formatter board and a DMD board (right-hand side of Fig. 1). The formatter board receives the images from a computer and handle DMD image processing. There is a notable difference that separates this system from other DMD board designs; as the DMD board is fed through an FPGA. This enables splitting the DMD into five zones with each zone being driven with a different pattern and refresh rate. This functionality reduces the number of test vehicles and test duration because several conditions can be tested in parallel on the same DMD. The DMD board contains the DMD and two TI chips controlling the reset drivers control signals.

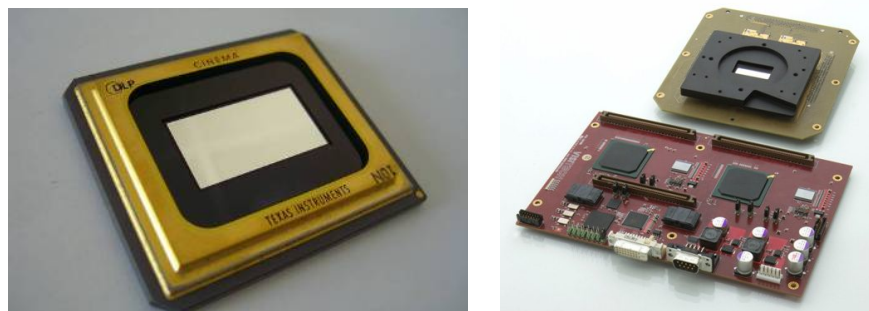


Fig. 1. DMD chip from Texas Instruments (2048 x 1080 micromirrors); formatter and DMD boards.

The electronic test vehicles were designed by Visitech for extreme test conditions using essentially commercial off the shelf components. In addition, the EUCLID operation requires that each DMD micromirror will be held in one position for 1500 seconds at a time. The DMD board has no protective coating or printed reference designators that can cause outgassing. All components on the DMD board were selected in an attempt to avoid outgassing materials. Careful layout of the components on the electronics boards allowed for efficient shielding of active components that should not be radiation tested. Current sense resistors enabled current measurements during and in between radiation testing.

### III. COLD TEMPERATURE TEST EQUIPMENT AND PROCEDURE

The Laboratoire d'Astrophysique de Marseille has over the last few years developed an expertise in the characterization of micro-optical components [7,8,9]. This expertise in small-scale surface deformation characterization of micro-optical components as well as operational testing of MOEMS components has been used for developing a dedicated cold temperature test set-up for DMD measurements in EUCLID operating conditions.

#### A. Cryostat & optical bench

For environmental testing (vacuum and low temperature), a cryostat has been developed at LAM. The bench (Fig. 2) is used as a photometric bench. In order to get enough resolution on each micromirror, the FOV images approximately 200x200 micromirrors onto a 1k x 1k camera. To inspect the complete DMD, a stitching procedure is carried out, by means of motorized stages. For the sake of test accuracy and efficiency, the characterization set-up is automated as much as possible. Three computers are used for managing the tests. The thermal chamber enables tests in a vacuum environment with temperature adjustment in the range of -60°C to +20°C. Temperature change is obtained through a liquid cooler.

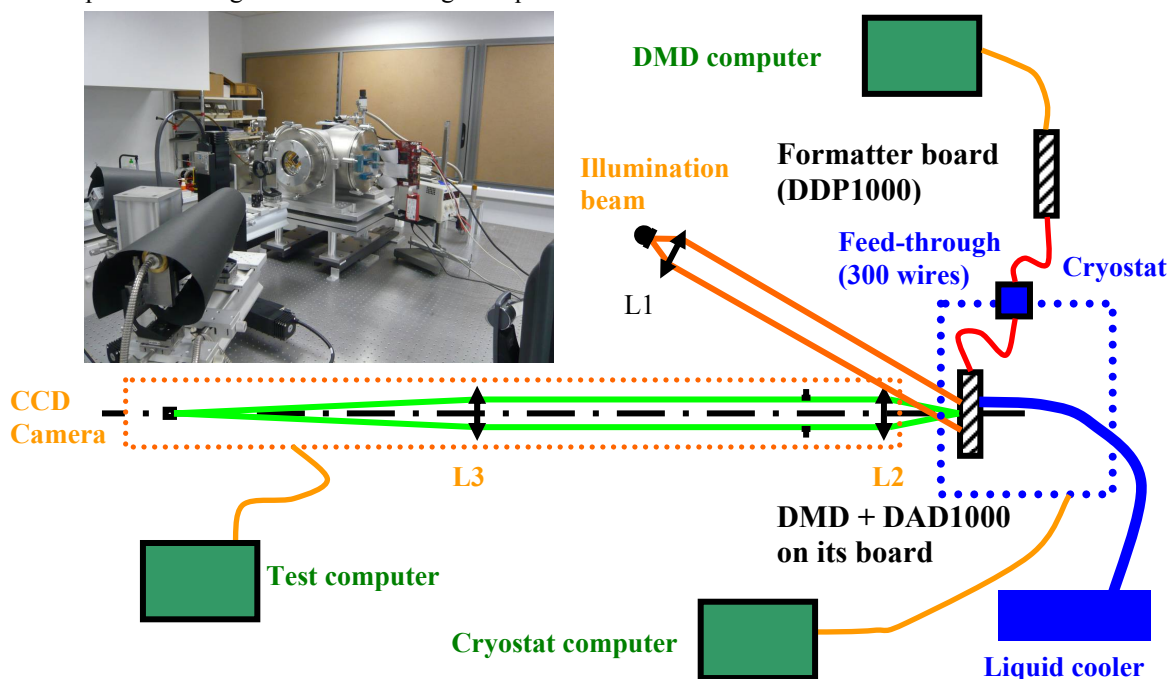


Fig. 2. Cold temperature test set-up

The DMD board is mounted in the chamber and linked by 300 wires through the chamber to the formatter board. The optical system is diffraction limited on the detector, leading to an optimized photometric measurement. The device is divided into **50 zones**. The FOV to be imaged by the CCD camera covers one zone, equivalent to **205 x 216 micromirrors** (44280 micromirrors). The plate scale on the 1k x 1k camera is exactly 4.07 x 4.07 detector pixels / micromirror. For complete DMD testing, the stitching procedure is done by means of motorized stages in three directions (XYZ). All software is developed in Matlab.

### B. Device driving

Hardware and software were developed by Visitech and LAM for driving the DMD boards. The hardware is controlled by a RS-232 serial link and a DVI port is used for loading an image onto the DMD. The software is developed in Matlab for driving the DMD chip. In order to test extensively the DMD devices, each component has been divided into 5 horizontal rows and each row can be driven in normal display-type mode or static modes (Fig. 3). This allows for testing of all modes on a single DMD at the same time. 4/5 of the DMD operates in a static ON or OFF mode (arbitrary pattern) and 1/5 of the DMD operates in display-type mode where the pattern is updated at 1Hz rate. This results in a display-type zone of roughly 400 000 micromirrors and static zones of 4 times this size, which is an ample amount for statistical analysis of the test results. Each pattern row is divided in 10 zones for a total of 50 zones, and each zone is imaged on the CCD camera (central picture of Fig. 3). The individual patterns show lines with different width and orientation, chessboard features and MOS-like patterns. Each micromirror is imaged on the CCD camera on about 4x4 detector pixels, which is enough for monitoring and detection of failures (if any) during the tests. A zoom on the area simulating a MOS-like pattern, with multi-slits is shown in right-hand side of Fig. 3. Any slit location and shape can be generated. It has to be noticed that the OFF mirrors cannot be imaged on the detector due to the high contrast performance of DMD.

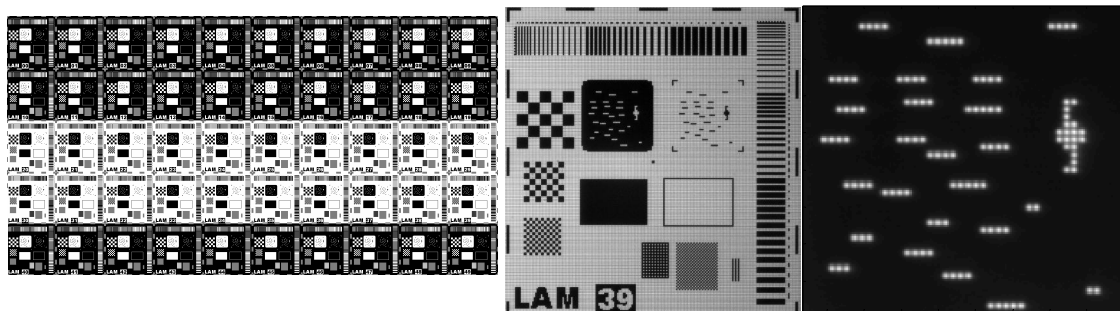


Fig. 3. LAM designed pattern; Image of a zone taken with the characterization set-up CCD camera and close-up view on a MOS-like pattern

### C. Analysis procedure

A data pipeline for data reduction has been developed using Matlab software. Photometric measurements are done before, during and after each test, and compared to the reference measurements (taken before the test, at room temperature). Any degradation in performance of a mirror will be revealed. We have adopted three mirror degradation definitions: - the **blocked mirror** when the mirror is non-responsive (e.g. "stuck"), - the **lossy mirror** when the optical throughput is decreased by more than 20%, and - the **weak mirror** when the optical throughput is decreased between 10% and 20%. For automatically detecting these mirrors, we have defined two parameters: **micro-mirror average throughput calculation** and **centroid calculation**. The micro-mirror average throughput is the flux integrated in the area of each micro-mirror. The centroid is calculated within the area of the micro-mirror and located on the map: for blocked mirrors, there is a major shift while for lossy mirrors, the shift is small. There is nearly no shift for weak mirrors. We have developed software for an automatic analysis of all data recorded during our measurements. All failure types are searched and detected, and results are displayed into maps and graphs, after removing false failure detections. The false failure detections are due mainly to dust particles present on the camera or the DMD window. The final results are then given in three graphs (example: Fig. 4) showing the number and the locations of failed mirrors (blocked, lossy and weak). All fifty zones from the DMD are shown in a matrix pattern (zone 00 to zone 49), and the number of affected mirrors is assigned to each zone. Comparison of measurements before and after testing shows the evolution of the failure rate.

## IV. COLD TEMPERATURE TEST

### A. Cold temperature step stress test and nominal cold temperature test

The cold temperature step stress test has been done from room temperature down to -60°C. **This test shows that permanent failure, i. e. stuck mirrors, is appearing on some mirrors when the device is taken down to -55°C.** The failure rate increases at -60°C. **Based on these results, the nominal temperature condition for**

**EUCLID was set to -40°C.** In order to confirm that this is an acceptable nominal operating condition for the device, a single DMD was tested. The DMD was mounted in the cold temperature chamber and tested three times at this temperature. For minimizing stress on the device when cooling down, a fast (-40°C / hour) and homogeneous cooling was provided. Using the definitions of blocked, lossy and weak mirrors, we have analyzed all (over 2 million) mirrors from the DMD for each measurement. No blocked mirror was revealed while only 12 mirrors are defined as lossy, and between 3 to 7 as weak mirrors. According to the screening procedure of TI where all mirrors are considered to be either working or not working, this measurement shows intermediate states where lossy and weak mirrors are observed; lossy mirrors stay lossy during the whole test, and weak mirrors may change in status from test to test; all other mirrors show their full performances. This effect is possibly due to local non-uniformity at individual mirror level, present since device fabrication. We highlight the fact that these effects have no impact in a typical DMD display mode, but they have to be taken into consideration and calibrated for MOS application. These numbers are very low when compared to the total 2 millions mirrors operating in the device. **This test revealed no degradation of the device when three consecutive cycles in EUCLID conditions are applied.** The cold temperature step stress test and the nominal cold temperature test have been fully described previously [10].

*B. Thermal cycling*

Thermal cycling has been done on one DMD, and conducted at INAF/IASF's facility in Bologna in Italy. An Angelantoni ACS Challenger 250 Climatic chamber located in a class 100.000 clean room was used for the 562 thermal cycles. Two sets of cycles (249 and 313 cycles) have been applied, with intermediate and final optical characterization. No anomaly was observed on the DMD by visual inspection: in particular no cracks, no flakes were observed. The results for the reference measurement at +20°C are 1 blocked, 4 lossy, and 15 weak mirrors. The results for the measurement at -40°C after the first serial of 254 cycles are 1 blocked, 2 lossy, and 7 weak mirrors. The results for the third measurement at -40°C after the second serial of 313 cycles are 0 blocked, 6 lossy, and 30 weak mirrors. Either one or zero blocked mirror is observed during this test, located in zone 13. The measured throughput is at the limit between blocked and lossy mirror. The number of weak mirrors is in the same range before and after testing; a slight increase of this number could be due to the extra dirt on the window. **In conclusion of the thermal cycling, this test has been successfully completed. This shows that space conditions did not degrade the device performances, within this thermal cycling campaign.**

*C. Life test*

The life test has been completed on one DMD device. The device was tested in EUCLID conditions, this means in vacuum, at -40°C and the device was operating with the following test cycle: pattern 1 is applied for 1500s (central pattern row is tilting in display mode while other pattern rows display a static pattern), the whole device is switching between pattern 1 and pattern 2 for 60s, and pattern 2 is applied for 1500s (central pattern row is tilting in display mode while other pattern rows display a static pattern). By this way, there is an identical duty cycle for all mirrors. **The life test lasted for 1038 hours.** Full optical tests were done during the whole life test. Measurements were done at room temperature (reference measurement), a first test at cold temperature was done at T0, then 11 intermediate measurements were done, and finally, a last measurement was done at the end of the life test, after **1038h**.

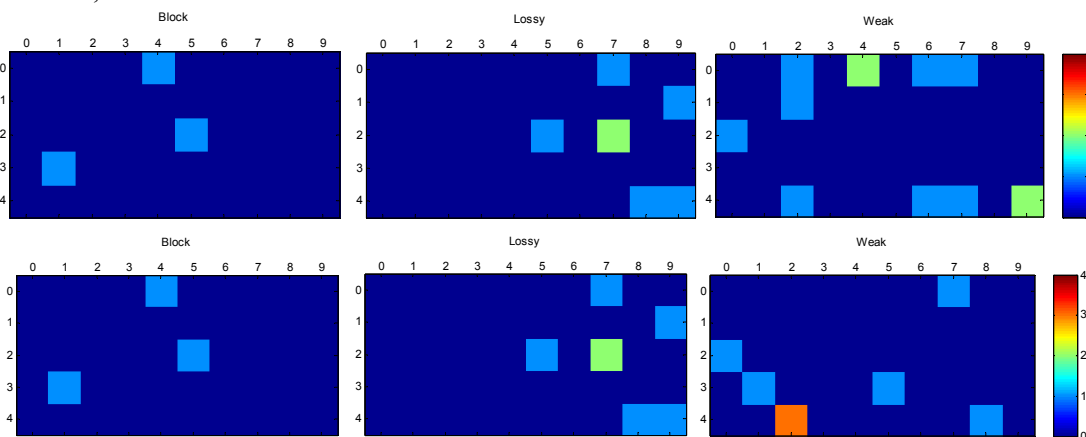


**Fig. 4.** First row: Location and numbers of affected mirrors at +20°C.

Second row: Location and numbers of affected mirrors at -40°C, after 1038 hours of life test.

After recording all data, we used the analysis procedure described in paragraph 3 for extracting the number and the locations of affected mirrors (blocked, lossy, weak). The results for the reference measurement at +20°C are presented in Fig. 4 first row in three graphs showing the number and the locations of affected mirrors with

3 blocked, 7 lossy and 12 weak mirrors. The results for the last measurement at  $-40^{\circ}\text{C}$  after 1038 hours of operation are shown in Fig. 4 second row with 3 blocked, 7 lossy and 8 weak mirrors. All intermediate tests are identical to these results with very little variation of only few mirrors for the weak case. From these charts, we clearly see that the same behavior is occurring for mirrors switching frequently (display mode in the central row) or in a static pattern during 1500s (EUCLID conditions), in the four other rows.

In conclusion of the life test, this test has been successfully completed. Three blocked mirrors and five lossy mirrors have been observed, but they are detected at ambient, at cold temperature at the beginning of the test and at cold temperature at the end of the test; they are not a consequence of the space conditions applied to the device. Other affected mirrors are only weak mirrors and their number is very low, with no increase while the life test is running. **This shows that space conditions did not degrade the device performances, within this life test period.**

## V. TID AND PROTON SEE RADIATION TESTING

### A. Total Ionizing Dose (TID) test

A complete test vehicle was in operation during the radiation testing, but by carefully shielding the test vehicle with lead bricks, only selected devices (DMD and electronics components) received a significant radiation dose. During the radiation testing the DMD displayed full black and full white test patterns that alternated every 1500 seconds. This is similar to the expected EUCLID duty cycle. A data logger measured the current consumption of major power supplies of the DMD chip set during radiation and provided the opportunity to monitor if and when any of the devices were degrading. **Total Ionizing Dose (TID) radiation tests established a tolerance level of 10 - 15 Krads for the DMD; at mission level, this limitation could likely be overcome by shielding the device.** The TID test has been fully described previously [10]. Optical characterizations were done on the samples before and the day after the radiation. An additional test was carried out one week later in order to measure longer term effect. No blocked mirror and five lossy mirrors have been observed before and after TID radiations; all lossy mirrors being at the same location. Other affected mirrors are weak mirrors and their number is low (around 30 mirrors), with no increase after the test. **We can then conclude that these results show that space conditions did not degrade the device performances, within this TID radiations test conditions.**

### B. Proton Single Event Effects (SEE) radiation test

The proton radiation test has been performed at the KVI facility in the Netherlands. During proton radiation, a live optical characterization has been conducted on a limited FOV around the center of the radiation beam hitting the device. The optical set-up is based on the set-up used in Marseille for observing the individual micro-mirrors with enough spatial resolution during the radiation process. The conditions for the first run was a 48 MeV beam from the accelerator, leading to 34.7 MeV on the DMD. The radiation started at low flux ( $6 \cdot 10^5$  p/cm<sup>2</sup>/s for 300s) and was to be increased to a higher flux ( $5 \cdot 10^7$  p/cm<sup>2</sup>/s for 896s) in order to reach a total dose of 10 Krads on the DMD. The proton radiation testing was unfortunately ended prematurely because of a break down in the accelerator after 120 seconds of radiation at low flux. **The lack of observed single events upsets is promising, but considering the length of the test, no conclusions can be made on the tolerance of the test vehicle in regards to single events upsets.**

## VI. VIBRATIONS AND SHOCKS

Mechanical vibration testing has been done on one DMD, and was conducted at ESTEC's facility in Noordwijk, the Netherlands. For this test, the standards MIL-STD-883F, methods 2005 (vibration fatigue) and 2007 (vibration at variable frequency) condition A, are followed: 20g during 32hours on each axis for vibration fatigue, and 20g at 20-2000Hz, 4 times on each axis for vibration at variable frequency. A special frame was manufactured to hold the DMD during the test and a double sided tape was used as an interface between the aluminium support and the ceramic package of the device which is very brittle. The vibration testing resulted in no visual effects that could be seen on the tested devices. The optical characterizations have been performed at LAM's facility. The results for the reference measurement at  $+20^{\circ}\text{C}$ , before vibrations, are 0 blocked, 2 lossy and 8 weak mirrors. The results after vibrations, at  $-40^{\circ}\text{C}$ , are 0 blocked, 1 lossy and 9 weak mirrors. No blocked mirror and one lossy mirror have been observed before and after vibrations (at  $-40^{\circ}\text{C}$  after vibrations). A second lossy mirror before vibrations is no longer visible after vibrations. Other affected mirrors are weak mirrors and their number is very low, with no increase after the test. **This shows that space conditions did not degrade the device performances, within this vibrations test conditions.**

Mechanical shock testing has been done on one DMD, and was conducted at ESTEC's facility in Noordwijk, the Netherlands. Shock test condition B of the MIL-STD-883f Method 2002 was applied on one DMD during

shock testing. It consists of a shock with a peak acceleration of 1500g and pulse duration equal to 0.5ms, 5 times on each axis. The device is fixed on a mass which is dropped in free fall against a stopper. A control accelerometer is fixed on the support and the acceleration profile during the shock is monitored. The shock testing resulted in no visual effects that could be seen on the tested vehicles. The optical characterizations have been performed at LAM's facility. The results for the reference measurement at +20°C (before shocks) are 0 blocked, 3 lossy and 7 weak mirrors. The results after shocks, at -40°C, are 0 blocked, 3 lossy and 6 weak mirrors. No blocked mirror and three lossy mirrors have been observed before and after shocks (at -40°C after shocks), at the same locations. Other affected mirrors are weak mirrors and their number is very low, with no increase after the test. **This shows that space conditions did not degrade the device performances, within this shock test conditions.**

## VII. CONCLUSION

Large field of view surveys with a high density of objects such as high-z galaxies or stars, such as in ESA EUCLID mission, benefit of multi-object spectroscopy (MOS) technique. Digital Micromirror Devices (DMD) could act as objects selection reconfigurable mask. ESA has engaged with Visitech and LAM in a technical assessment of using a DMD from Texas Instruments (2048 x 1080 mirrors on a 13.68µm mirror pitch) for space applications. Specialized driving electronics and a cold temperature test set-up have been developed.

Our tests reveal that the DMD remains fully operational at -40°C and in vacuum. The 1038 hours life test in space survey conditions (-40°C and vacuum), has been successfully completed. The device was operating continuously with typical MOS patterns. The numbers of affected mirrors are very low compared to the 2 million mirrors of the DMD array. Total Ionizing Dose (TID) radiation tests established a tolerance level of 10 - 15 Krads for the DMD; at mission level, this limitation could likely be overcome by shielding the device. Finally, thermal cycling (over 500 cycles between room temperature and cold temperature, on a non-operating device) and vibration and shock tests have also been done; no degradation is observed from the optical measurements. **These results do not reveal any show-stopper concerning the ability of the DMD to meet environmental space requirements.** Insertion of such devices into final flight hardware would still require additional efforts such as development of space compatible electronics, and original opto-mechanical design of the instrument.

From an ESA perspective, the micromirror arrays have therefore achieved a reasonable TRL (Technology Readiness Level). Insertion of such devices into final flight hardware would still require additional efforts (estimation is approximately 2 years) in terms of change of the window coating, re-development of space compatible electronics as well as a different package interface compatible with spacecraft launch conditions.

## ACKNOWLEDGEMENT

The authors thank Jean-Antoine Benedetti, Philippe Laurent and Vincent Herault from LAM for their assistance during the tests. This work is partly funded by ESA, CNRS, Provence-Alpes-Cote d'Azur regional council and Conseil General des Bouches-du-Rhone county council.

## REFERENCES

- [1] R. Burg, P.Y. Bely, B. Woodruff, J. MacKenty, M. Stiavelli, S. Casertano, C. McCreight and A. Hoffman, "Yardstick integrated science instrument module concept for NGST", in *Proceedings of the SPIE conference on Space Telescope and Instruments V*, SPIE **3356**, 98-105, Kona, Hawaii, 1998
- [2] F. Zamkotsian, K. Dohlen, D. Burgarella, V. Buat, "Aspects of MMA for MOS: optical modeling and surface characterization, spectrograph optical design", in *Proceedings of the NASA conference on "NGST Science and Technology Exposition"*, ASP Conf. Ser. **207**, 218-224, Hyannis, USA, 1999
- [3] M. Robberto, A. Cimatti, A. Jacobsen, F. Zamkotsian, F. M. Zerbi, "Applications of DMDs for Astrophysical Research", in *Proceedings of the SPIE conference on MOEMS 2009*, Proc. SPIE **7210**, San Jose, USA (2009)
- [4] M. J. Li; A. D. Brown; A. S. Kutlyrev; H. S. Moseley; V. Mikula, "JWST microshutter array system and beyond", Proc. SPIE 7594, San Francisco, USA, 2010
- [5] M. Canonica, S. Waldis, F. Zamkotsian, P. Lanzoni, W. Noell, N. de Rooij, "Development of MEMS-based programmable slit mask for multi-object spectroscopy", in *Proceedings of the SPIE conference on Astronomical Telescopes and Instrumentation*, Proc. SPIE **7739**, San Diego, USA (2010)
- [6] F. Zamkotsian, K. Dohlen, "Performance modeling of JWST Near Infrared Multi-Object Spectrograph," in *Proceedings of the SPIE conference on Astronomical Telescopes and Instrumentation 2004*, Proc. SPIE **5487**, Glasgow, United Kingdom (2004)
- [7] F. Zamkotsian, J. Gautier, P. Lanzoni, "Characterization of MOEMS devices for the instrumentation of Next Generation Space Telescope," in *Proceedings of the SPIE conference on MOEMS 2003*, Proc. SPIE **4980**, San Jose, USA (2003)
- [8] F. Zamkotsian and K. Dohlen, "Surface characterization of micro-optical components by Foucault's knife-edge method: the case of a micro-mirror array", *Applied Optics*, **38** (31), 6532-6539 (1999)
- [9] A. Liotard, F. Zamkotsian, "Static and dynamic micro-deformable mirror characterization by phase-shifting and time-averaged interferometry", in *Proceedings of the SPIE conference on Astronomical Telescopes and Instrumentation 2004*, Proc. SPIE **5494**, Glasgow, United Kingdom (2004)
- [10] F. Zamkotsian, E. Grassi, P. Lanzoni, R. Barette, C. Fabron, K. Tangen, L. Marchand, L. Duvet "DMD chip space evaluation for ESA EUCLID mission," in *Proceedings of the SPIE conference on MOEMS 2010*, Proc. SPIE **7596**, San Francisco, USA (2010)